Proceedings of the 21st ICSMGE, Vienna, Austria, 14 – 19 June 2026. Pistrol, Adam & Schweiger (eds.)
Published by: ÖGG, Austrian Society for Geomechanics, Salzburg, Austria, ISBN 978-3-9503898-4-5
https://doi.org/10.53243/ICSMGE2026-1361

Study of the bored pile side resistance in rock

Rafael Sharafutdinov
Gersevanov Research Institute of Bases and Underground Structures (NIIOSP) Research Center of Construction JSC, Moscow, Russia, linegeo@mail.ru

Dmitrii Botanin
Ural Federal University, Yekaterinburg, Russia, botanindp@gmail.com

ABSTRACT: Bored piles embedded in rock or cut through it are often utilized as foundation for high-rise buildings. As experience shows, the resistance of bored piles is mainly provided by the shaft surface. The value of the pile shaft resistance depends on the type of rock, strength of rock, shaft roughness, and the strain level during testing. Most of the methods for assessing bored pile resistance proposed in the literature consider only the unconfined compressive strength of the rock and do not account for the pile strain under load or the roughness of the pile shaft. This article presents the results of in-situ tests demonstrating the dependence of shaft resistance on the unconfined stress of the rock and the roughness of the shaft. Recommendations for evaluating the bearing capacity and conducting load tests for bored piles in rocky soils are given.

KEYWORDS: Bored pile, side resistance, rock

1 INTRODUCTION

The bearing capacity of bored piles is determined by both their side surface and base resistances. However, testing has demonstrated that the resistance of bored piles primarily comes from the side surface. Base resistance is typically engaged only after considerable displacement of the pile, which leads to failure of the side surface. Research by Horvath et al. (1979, 1983) showed that the side surface resistance of large-diameter piles can be mobilized with displacements of approximately 5-6 mm. Ng et al. (2001) found that for at *S/D* of ≤0.4%, the pile exhibits elastic behavior under working loads. Additionally, the load-displacement relationship becomes nonlinear, with full mobilization of side resistance occurring at around *S/D* ≈ 1%. However, pile base resistance begins to mobilize at *S/D* ≈ 5% (O'Neill et al., 1996). Numerous pile test results indicate that such displacement values are rarely achieved in rocks. Therefore, the bearing capacity of piles in rock masses is primarily derived from their side surface resistance.

The article presents an analysis of over 200 large-scale pile load tests conducted in various rock soils across construction sites in Russia, the USA, Canada, Hong Kong, Turkey, and other regions. The test loads reached up to 33.3 MN. A classification system based on a strain index was proposed, correlating to differential pile displacement. The study established the ranges of mobilized side resistance for piles associated with different strain indices. Additionally, it determined the relationship between the side resistance of bored piles and both the uniaxial compressive strength of the rock and the strain value.

2 DETERMINING THE SIDE SURFACE RESISTANCE OF BORED PILES

The side surface resistance of bored piles in rock, denoted as f_s, can be determined using the following straightforward equation:

$$\frac{f_s}{p_a} = \alpha \left(\frac{R_c}{p_a}\right)^m \quad (1)$$

where R_c is unconfined compressive strength, p_a = 0.1 MPa is atmosphere pressure, α and *m* are empirical coefficients.

This empirical dependence was proposed by Rosenberg and Journeaux in 1976, based on extensive large-scale pile tests. In 1978, Horvath analyzed databases of pile and anchor test results, primarily conducted in sedimentary rocks. Subsequently, in 1983, Horvath et al. established a relationship between side resistance (f_s) and the strength of the weaker material (either pile concrete or rock) through experimental data analysis. Rowe and Armitage conducted a review in 1984, examining over 70 bored pile test results with diameters ranging from 0.064 m to 1.300 m. Employing this dataset, Carter and Kulhawy in 1988 derived empirical coefficients α and m as a lower bound with a significance level of 0.9. In 1999, Reese and O'Neill analyzed the aforementioned dependencies and proposed their correlation. Zhang and Einstein also reviewed existing databases and the correlations between f_s and R_c established by other researchers in 1998, leading to their own proposed coefficients. They further expanded their study in 1999, refining the correlation coefficients to align more closely with those of Carter and Kulhawy (1988). In 2001, Ng et al. reviewed available databases and conducted tests on bored piles in Hong Kong, resulting in their own proposed relationship. Finally, Kulhawy et al. conducted another evaluation of these dependencies in 2005, concluding that most authors adopted m=0.5, while their additional research estimated the coefficient α to be 1.0. Table 1 summarizes the dependencies presented by the authors mentioned above.

Table 1. Empirical coefficients α and m for equation (1)

Authors	α	*m*
Rosenberg и Journeaux, 1976	1.19	0.52
Horvath, Kenney, Kozicki, 1983	0.63-0.95	0.5
Rowe и Armitage, 1984	1.42	0.5
Carter и Kulhawy, 1988	0.63	0.5
Reese и O'Neill, 1999	0.65	0.5
Zhang и Einstein, 1998	1.26	0,5
Zhang и Einstein, 1999	0,63	0.5
Ng, Yau, Li, 2001	0.6	0.5
Kulhawy, Prakoso, Akbas, 2005	1	0.5

Analysis indicates that many current methods for estimating the side surface resistance of piles are based on the unconfined compressive strength of the rock and do not take into account the strain experienced by the pile. In practice, pile tests conducted in rocky conditions are typically performed at relatively low loads, which prevents an accurate assessment of their true (maximum) bearing capacity. Consequently, most pile solutions incorporate significant design margins, presenting opportunities for optimization in project design.

3 OVERALL DESCRIPTION OF THE ROCKS AND PILES UNDER INVESTIGATION

The experimental data comprised results from a series of pile tests assessing compression and pull-out loads, gathered from various construction sites in Russia, Turkey, the USA, and other countries. Table 2 presents the characteristics of the rocks and piles from these sites. The rocks examined in this study included shale, limestone, sandstone, gabbro, granite, and porphyrite, among others.

The unconfined compressive strength ranged from 0.23 to 55.0 MPa. The bored piles tested had diameters between 0.43 and 1.83 m, with embedded lengths varying from 0.5 to 22.2 m. The maximum test loads reached up to 33.3 MN. The maximum pile displacement (S) ranged from 0.12 to 130.0 mm, which enabled the measurement of mobilized side surface resistance (f_{sm}) between 0.01 and 5.40 MPa.

Table 2. Summary of pile test results in rocky soils summarized by the authors (Sharafutdinov R.F., Botanin D.P., 2024)

Site location	Rock type	Rock	N	d, m	L, m	R_c, MPa	Q, MN	S, mm	f_{sm}, MPa
Russia, Ekaterinburg	Magmatic	Gabbro	9	0.8	0.50-4.50	6.3-27.8	2.7-4.4	8.04-54.56	0.24-2.90
Russia, Ekaterinburg		Granite	33	0.62-1.0	0.51-5.19	2.2-37.1	4.1-4.4	0.12-21.69	0.06-3.61
Russia, Ekaterinburg		Porphyrite	12	0.43-0.8	0.50-2.06	2.00-25.20	0.4-4.4	4.71-51.81	0.06-2.91
Russia, Ekaterinburg	Metamorphic	Shale	31	0.62-0.8	1.4-22.2	2.5-28.4	0.6-7.4	0.84-111.16	0.03-1.58
Russia, Moscow	Sedimentary	Limestone	36	0.9-1.5	0.6-14.8	3,0-55,0	12.0-33.3	1.33-130.0	0.10-5.40
Russia, Kemerovo		Sandstone	4	0.75	6.0-7.6	28.5	7.1-7.3	5.2-11.85	0.40-0.50
Turkey (Akguner and Kirkit, 2012)	Sedimentary, metamorphic	Argillite, marl, sandstone, shale, phyllite	7	0.8-0.9	1.5-16.0	0.8-2.2	5.5-12.0	3.05-42.1	0.09-1.18
USA (Castelli and Fan, 2002)	Sedimentary	Limestone, marl	5	0.92-1.83	4.75-6.58	0.7-7.5	-	5.8-24.0	0.38-1.24
USA (Brown D.A., Turner J.P., Castelli R.G., 2010)	Sedimentary	Siltstone, argillite, sandstone	25	0.51-1.83	0.6-11.0	0.15-54.9	-	0.51-53.09	0.1-2.6
Great Britain, USA, Australia, Canada (M.W. O'Neill et al, 1996)	Magmatic, sedimentary, metamorphic	Siltstone, basalt, chalk, marl, shale, argillite, sandstone	63	0.46-1.60	0.9-18.0	0.23-14.74	-	0.76-10.16*	0.01-1.51

Note: n – number of tests; d – diameter; L – rock embedment; R_c – unconfined compressive rock strength; Q – maximum pile test load; S_{max} – maximum displacement of the tested pile; f_s – measured mobilized side surface pile resistance; *– precipitation is given for 50% of the maximum load

4 METHODS AND RESULTS

The statistical analysis of correlation and regression was conducted using MS Excel and IBM SPSS Statistics. The following bearing capacity parameters were examined:

- Mobilized side surface resistance (f_{sm}).
- Normalized mobilized side surface resistance (f_{sm}/p_a).
- Ratio of mobilized side surface resistance to unconfined compressive strength (f_{sm}/R_c).
- Ratio of pile displacement to pile embedment in rock (relative pile strain, S/L_r).
- Ratio of pile displacement to pile diameter (S/D).

Experimental studies were conducted in two stages.

In the first stage, the experimental data were integrated into the overall sample. Statistical analysis was performed to calculate Pearson's correlation coefficient (ρ), significance level (using P-value), and the sample correlation ratio (η) as described by Gmurman V. (2004).

Pearson's correlation coefficient (ρ) widely used in statistical analysis assesses the strength and direction of the linear relationship between parameters, with values ranging from -1 to +1. A value close to +1 (or -1) indicates a strong linear relationship, while a value near zero suggests a weak linear strength relationship between the parameters.

The correlation parameter η represents the ratio of between-group dispersion to total dispersion. It quantifies the strength of the non-linear correlation between parameters, with values ranging from zero to one. A value near zero indicates a weak or nonexistent relationship, while a value close to one signifies a strong relationship. Additionally, the correlation ratio and Pearson's correlation coefficient satisfy the condition $\eta \geq \rho$.

The correlation analysis identified the most significant factors and the nature of their relationships, whether linear or non-linear. The analysis of correlation interactions was conducted at a significance level of $\alpha = 0.05$, in accordance with GOST 20522 standards for calculating the soil safety factor.

The following factors that may influence the bearing capacity of bored piles in rock were examined:

- Unconfined compressive rock strength (R_c).
- Normalized unconfined compressive rock strength (R_c/p_a).

- Relative depth of pile embedment in rock (L_r/D).
- Pile displacement in rock (S).
- Ratio of pile displacement to pile embedment in rock (S/L_r).
- Ratio of pile displacement to pile diameter (S/D).

The key findings from the correlation analysis of the overall data set are presented in Table 3. It is noteworthy that the relationships among the parameters analyzed are both significant and highly non-linear.

Table 3. Correlation parameters for the total sample

Bearing capacity parameter		Factor					
		R_c	R_c/p_a	L_r/D	S	S/D	S/L_r
f_{sm}	ρ	0.720*	0.720*	-0.462*	0.110	0.075	0.386*
	η	0.937	0.937	0.974	0.938	0.950	0.999
f_{sm}/p_a	ρ	0.720*	0.720*	-0.462*	0.110	0.075	0.386*
	η	0.937	0.937	0.974	0.938	0.950	0.999
f_{sm}/R_c	ρ	-0.315*	-0.315*	-0.118	-0.086	-0.095	0.070
	η	0.981	0.981	0.790	0.901	0.935	0.997
S/L_r	ρ	0.191*	0.191*	-0.328*	0.668*	0.616*	–
	η	0.754	0.754	0.841	0.967	0.969	–
S/D	ρ	0.028	0.028	-0.043	0.897*	–	–
	η	0.624	0.624	0.941	0.999	–	–

* – correlation is significant at the significance level α=0.05

Sample size N=228

The analysis indicated that the unconfined compressive rock strength (R_c) and the ratio R_c/p_a (see Figure 1), along with the length of embedment in rocky soils (L_r/D), significantly affect the mobilized pile side surface resistance (f_{sm}) and its ratio to p_a (f_{sm}/p_a). Non-linear behavior is predominant in this context, with η exceeding ρ by a factor of 1.3 to 2.1.

Conversely, the relationships between mobilized side surface resistance and pile displacements (S and S/D) are weak and statistically insignificant. However, the ratio S/L_r does influence the mobilized resistance (f_{sm} and f_{sm}/p_a) and is inversely related to the embedment length in the rock (L_r/D).

Based on the analysis performed of the total sample, the following conclusions can be drawn:

- The mobilized side surface resistance of piles is influenced by soil strength, the length of pile embedment in rock, and the S/L_r ratio.
- The mobilized pile resistance is insignificantly affected by pile displacement (S) and the displacement-to-diameter ratio (S/D).

In the second stage, a detailed examination was conducted on how rock strength and pile displacement affect the mobilized side surface resistance of piles.

Randolph (1994) noted that full mobilization of the side surface occurs at an S/D ratio of 1%. Based on this ratio, Ng et al. (2001) proposed a classification system for tested piles using a displacement index (DI), which serves as an approximate measure of the pile's "local" displacement and the extent of side resistance mobilization relative to the maximum side resistance value.

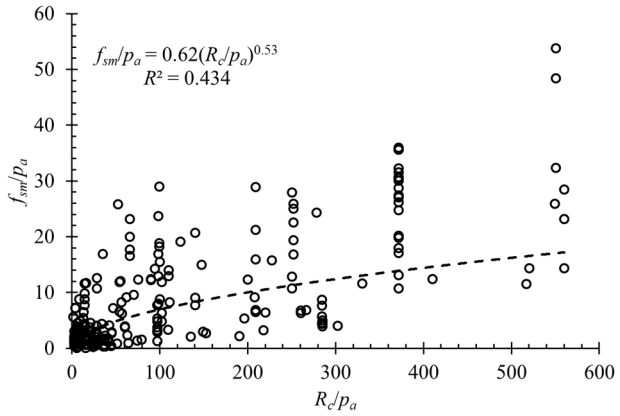

Figure 1. Relationship between normalized mobilized side surface resistance f_{sm}/p_a and normalized unconfined compressive strength R_c/p_a according to field tests

Index A is assigned to pile tests where S/D is greater than or equal to 1% and the f_{sm}/S ratio is less than 30 kPa/mm, indicating values of f_{sm} that are close to fully mobilized side resistance (Ng et al., 2001). Index B is designated for results with an S/D ratio between 0.4% and 1% and an f_{sm}/S ratio of less than 200 kPa/mm. Index C encompasses all remaining results.

A limitation of this classification method is that bored piles in rock typically exhibit minimal displacements, with most strains resulting from the compression of the pile material, particularly in longer piles (Gotman and Gavrikov, 2021). Furthermore, the DI does not account for strain in the pile material itself, and using f_{sm}/S for categorization may not always be appropriate, as the observed strain rates are often higher.

The correlation analysis indicated that the S/D ratio does not have a significant impact on f_{sm}. Additionally, both pile displacement and the measured f_{sm} resistance are heavily influenced by the length of the pile's embedment in the rock mass. The authors suggest that the relative pile strain, S/L_r, is a more appropriate measure for categorizing strain levels. This metric aligns with the classical definition of pile strain, as the width of the interaction zone between a single pile and the surrounding soil is comparable to the length of its embedment (Randolph, 1994; Fleming et al., 2009). Consequently, a new classification for pile strain, referred to as the strain index (SI), is proposed:

I – $S/Lr \geq 1\%$;

II – $0.5\% \leq S/Lr < 1\%$;

III – all other results.

This classification will facilitate a more accurate assessment of pile bearing capacity while excluding data associated with negligible strains.

Figure 2 shows the combined impact of R_c/p_a and SI on f_{sm}/p_a values. As S/L_r increases, the resistance f_{sm}/p_a also rises, while lower f_{sm}/p_a values are typically associated with minimal strain levels. This suggests that the relationships derived from this data exhibit significant safety margins.

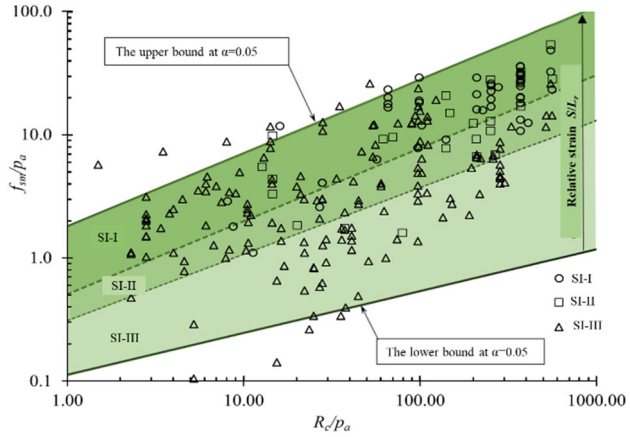

Figure 2. Effect of normalized unconfined compressive strength (R_c/p_a) on the normalized mobilized side surface resistance (f_{sm}/p_a) as a function of the strain index.

Figure 2 presents both a quantitative and qualitative evaluation of the effect of R_c/p_a on f_{sm}/p_a in dependence on the level of deformation. The obtained equation could be useful for practical applications:

$$\frac{f_{sm}}{p_a} = \alpha \left(\frac{R_c}{p_a}\right)^m \quad (2)$$

where α and m are empirical coefficients. The values of α and m are influenced by the strain index, with respective values of 0.77 and 0.6 for SI-I (R^2 = 0.68), 0.75 and 0.54 for SI-II (R^2 = 0.51), and 0.93 and 0.34 for SI-III (R^2 = 0.22).

The empirical coefficients obtained are largely consistent with those reported by other researchers (see Table 1). Notably, both the empirical coefficients and strain levels increase concurrently. Based on the analysis of a substantial total sample from pile load tests conducted in rock, the following semi-empirical dependence was proposed:

$$\frac{f_{sm}}{p_a} = a \left(\frac{S}{L_r}\right)^b \left(\frac{R_c}{p_a}\right)^c \quad (3)$$

The empirical coefficients a, b, and c are influenced by the genesis of the rock and are detailed in Table 4.

Equation (3) calculates the side surface resistance of a pile based on the anticipated strain level, which can be determined using established methodologies (Fedorovsky V., 1974; Randolph M. and Wroth C., 1978). Despite this approach, pile load testing remains essential. Furthermore, this dependence allows for a reduction in the excessive safety factors applied to the bearing capacity of piles which were derived from empirical dependences established from underloaded pile test results.

Table 4. Empirical regression coefficients for Equation (3) depending on rock type

Empirical coefficients	Total sample	MG	MT	SD
a	2.81	3.89	5.88	3.4
b	0.223	0.225	0.201	0.185
c	0.526	0.474	-0.723	0.468
R^2	0.665	0.750	0.514	0.56
N	228	62	71	95

Rock type: MG – magmatic; MT – metamorphic; SD – sedimentary

The equations (2) and (3) are based on empirical data obtained under conditions where failure on the pile side surface did not occur. While they provide a more accurate assessment of the pile surface resistance, they still have a significant safety factor.

To conduct a detailed study of pile side surface resistance and determine total side surface resistance, special laboratory pile shaft model tests were conducted. The pile shaft models consist of a combination of a model of a drilled pile with a diameter of 180 mm, with a preset roughness, and a model of rocky soil created using cement-sand grout (Figure 3). The models of piles were made from concrete B25 (concrete with unconfined compressive strength of 25 MPa). The model of rocky soils created using cement sand grout with compressive strength ranging from 0.3 to 28.0 MPa. The pile shaft models have the following characteristics:

- pile roughness profile corresponds to that of actual drilled pile;
- piles were equipped with to measure both vertical and horizontal strain and stress during loading;
- shaft models are included in a tube that simulates boundaries, which involve the suppression of dilatancy during the failure process.

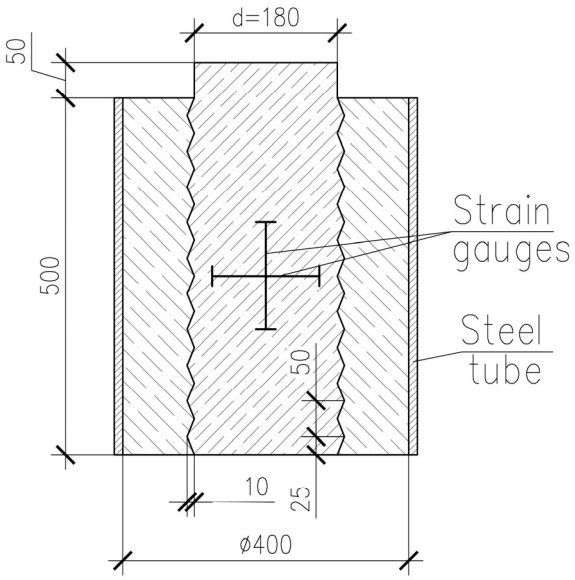

Figure 3. Scheme of the pile shaft model

The pile shaft model samples were installed in a special load frame and loaded up to the ultimate resistance of the pile shaft (0). Both the total displacements of the pile and the strain gauges indices were collected under loading.

0 shows the pile shaft model sample before and after testing. Failure was observed to occur along the side surface of the soil.

Figure 6 shows a typical graph of normal stresses on the pile surface as displacement increases.

Figure 4. Pile shaft model installed in a special load frame.

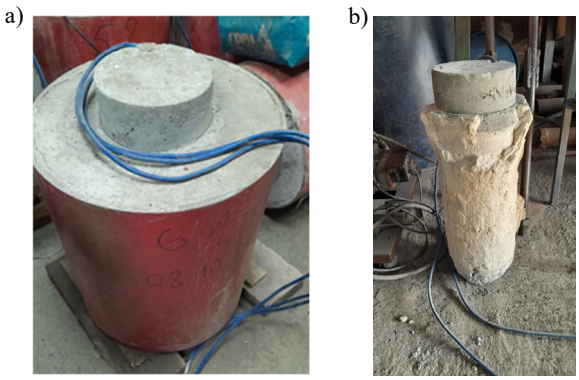

Figure 5. The pile shaft model before (a) and after (b) testing.

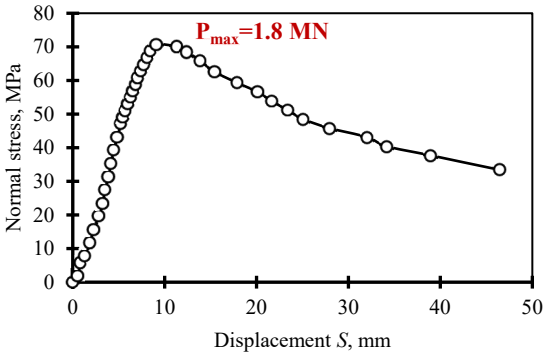

Figure 6. Typical graph of normal stresses on the pile surface with increasing displacement.

Based on the results from laboratory tests on the pile shaft model samples, a *fs/pa-Rc/pa* was plotted (see Figure 7). The laboratory findings indicate that the coefficients α and m in equation (2) are 6.3 and 0.51 respectively, assuming complete resistance along the side surface of piles.

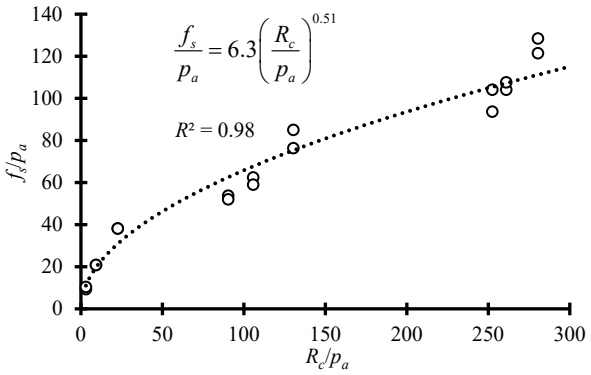

Figure 7. Relationship between normalized mobilized side surface resistance f_{sm}/p_a and normalized unconfined compressive strength R_c/p_a according to laboratory tests.

5 DICUSSION

The bearing capacity of bored piles, as determined through testing, is frequently assessed based on the mobilized side surface resistance. This resistance is influenced by the maximum load applied during the test and the strain experienced by the pile due to the loading.

The proposed strain index facilitates the analysis of mobilized resistance and helps estimate the failure load level of the pile. This index can also be utilized to evaluate f_{sm} of long and large-diameter piles in dispersed soils, particularly when the test load results in minimal displacements.

Consequently, the bearing capacity of bored piles in rock is often underestimated. This underestimation leads to significant safety margins in the design of pile foundations, ultimately resulting in increased construction costs for zero cycle work. Moreover, the f_{sm} value in rock depends upon the length of pile embedment. This is because the distribution of side stress along the pile in rock does not exceed the defined limits of stress transfer depth. Once these limits are exceeded, the side surface of piles practically stops transferring load.

To avoid excessive stockpiling, it is recommended to determine the maximum value of f_{sm}. This can be achieved by creating 2-3 meter long pile fragments at construction sites, which can then be tested to failure. An example of this method was utilized during the construction of the Ice Arena in Yekaterinburg (Sharafutdinov R. et al., 2022), resulting in a twofold reduction in the number of piles required.

Additionally, the proposed equation (3) can be employed to estimate the maximum f_{sm} value. By using established methods for calculating pile displacement, more precise resistance values can be determined iteratively. This dependence enhances the understanding of load transfer along the borehole pile shaft, taking into account both pile displacement and embedment depth in rock.

Overall, the empirical relationship obtained from both field and laboratory tests yields a coefficient α. In field tests this value is approximately 0.62, while in laboratory tests it equals 6.3. This ten-fold difference is primarily due to the fact the load on pile did not cause its failure during field tests at construction sites and actual ultimate resistance was not realized. Furthermore, natural deposits in real solid rocks feature joints and drilled solids at the "pile-soil" interface, which were not considered at this stage of laboratory studies.

6 CONCLUSIONS

This paper analyzes the results of over 200 large-scale pile-load tests conducted in various rock soils at construction sites across Russia, the USA, Canada, Hong Kong, Turkey, and other regions. Through correlation analysis, it has been determined that the mobilized side surface resistance of piles is influenced by soil strength, pile embedment length, and the differential pile displacement value S/L_r. Conversely, the absolute displacement values S and the displacement-to-diameter ratio S/D have minimal impact on the mobilized pile resistance.

A classification of bored piles based on the strain index related to differential pile displacement is proposed: SI-I for $S/L_r \geq 1\%$; SI-II for $0.5\% \leq S/L_r < 1\%$; and SI-III for all other results. This classification facilitates a more accurate assessment of the bearing capacity of piles in rock, helping to eliminate underestimated values of f_{sm} associated with negligible strains. Additionally, the ranges of mobilized side surface resistance for various strain indices have been established.

A combined dependence is also proposed to estimate the mobilized side surface resistance by taking into account both rock strength and pile strain. This approach enhances the understanding of load transfer through the lateral walls of the borehole, considering factors such as pile displacement and embedment depth in rock.

7 REFERENCES

Akguner C. and Kirkit M. 2012. Axial bearing capacity of socketed single cast-in-place piles. *Soils and Foundation* 52(1), 59–68.

Brown D.A., Turner J.P., Castelli R.G., 2010 Drilled shafts: construction procedures and LRFD design methods. *Report FHWA NHI-10-016*, National Highway Institute.

Carrubba P. 1997. Skin friction of large-diameter piles socketed into rock. *Can. Geotech. J*. 34, 230–240.

Carter J.P. and F.H. Kulhawy. 1988. Analysis and design of drilled shaft foundations socketed into rock. *Report EL-5918*, Palo Alto: Electric Power Research Institute.

Castelli R.G. and Ke Fan. 2002. O-Cell Test Results for Drilled Shafts in Marl and Limestone. *International Deep Foundations Congress*, ASCE, New York, 807–823.

Fedorovsky V.G. 1974. Calculation of pile settlements in homogeneous and multilayer foundations (*in Russian*). *PhD thesis in Engineering Science*, Moscow.

Gmurman V.E. 2004. Manual for solving problems in probability theory and mathematical statistics. (*in Russian*). Vyshaya Shkola, Moscow.

Gotman A.L. and Gavrikov M.D. 2021. Study of the peculiarities of vertically loaded long bored piles and their calculation. *Construction and Geotechnics*. 12 (3), 72–83. https://doi.org/10.15593/2224-9826/2021.3.08

Gunnik B. and Kiehne C. 1998. Pile bearing in Burlington Limestone. *Transportation conference proceedings*, 145-148.

Horvath R. G. and Kenney T. C. 1979. Shaft resistance of rock socketed drilled piers. *Proc. symposium on deep foundations*., ASCE, New York, 182–214.

Horvath R.G., T.C. Kenney and P. Kozicki. 1983. Methods of improving the performance of drilled piers in weak rock. *Canadian Geotech. J*. 20(4), 758-772

Fleming K., Weltman A., Randolph M, Elson K. 2009. *Piling Engineering*. Taylor & Francis, London and New York.

Kulhawy F.H. and Phoon K.K. 1993. Drilled shaft side resistance in clay soil to rock. *In Design and Performance of Deep Foundations: Piles and Piers in Soil and Soft Rock (GSP 38)*, ed. P.P. Nelson, T.D. Smith & E.C. Clukey, 172-183.

Kulhawy, F.H., Prakoso W.A., Akbas S.O, 2005. The 40th U.S. Symposium on Rock Mechanics, USA, Anchorage.

Mackiewicz S. M., Qmar O., Larsen J., 2008. Skin friction in shale: results of the HWY. 81 bridge, Yankton, SD drilled shaft load test. *Proceedings of the 33rd annual and 11th international conference on deep foundations*, 249-254.

McVay, M.C., F.C. Townsend & R.C. Williams. 1992. Design of socketed drilled shafts in limestone. *J. Geotech. Eng.(ASCE)*. 118(10), 1626-1637.

Ng C., Yau T., Li J., Tang W. 2001. Side Resistance of Large Diameter Bored Piles Socketed into Decomposed Rocks, Journal of Geotechnical and Geoenvironmental Engineering 127 (8), 642-657

O'Neill M.W., Townsend F.C., Hassan K.M., Buller A., Chan P.S. 1996. Load transfer for drilled shafts in intermediate geomaterials. *Report FHWA-RD-95-172*. Federal Highway Administration.

O'Neill, M.W. and Reese L.C. 1999. Drilled shafts: construction procedures and design methods. *Report FHWA-IF-99-025*. Federal Highway Administration.

Randolph M.F. 1994. Design methods for pile groups and piled rafts. *Proceeding of the XIII ICSMFE*. New Delhi, India, 61-82.

Randolph M.F., Wroth C.P. 1978. Analysis of Deformation of Vertically Loaded Piles. *Journal of the Geotechnical Engineering Division*, 104(12), 1465-1488.

Rosenberg P. and Journeaux N.L. 1976. Friction and end bearing tests on bedrock for high capacity socket design. *Canadian Geotech. J*. 13(3), 324-333.

Rowe R. K., Armitage H. H. 1984. Design of piles socketed tt weak rock. Report GEOT-11-84. London., Univ. of Western Ontario.

Randolph M.F., Wroth C.P. 1978. Analysis of Deformation of Vertically Loaded Piles. *Journal of the Geotechnical Engineering Division*, 104(12), 1465-1488.

Sharafutdinov R.F., Shulyatev O.A., Isaev O.N., Zakatov D.S. 2022. Studies of interaction of drilled piles with rocky soils. *Soil Mechanics and Foundation Engineering*, 59, 430-436. https://doi.org/10.1007/s11204-022-09833-4

Sharafutdinov R.F., Botanin D.P., Study of the Side Resistance of Bored Piles in Rock 2024. *Soil Mechanics and Foundation Engineering*, 61, 299-307. https://doi.org/10.1007/s11204-024-09976-6.

Shulyat'ev O.A., Sharafutdinov R.F. and Shulyat'ev S.O. 2022 Generalization of test results for drilled piles in rocky soils. *Soil Mechanics and Foundation Engineering*, 59, 1-6. https://doi.org/10.1007/s11204-022-09777-9.

Thorburn S. 1966. Large diameter piles founded on bedrock. *Proc., Symp. on Large Bored Piles, Institution of Civil Engineers*, London, 120–129.

Walter D. J., Burwash W. J. and Montgomery R. A. 1997. Design of large-diameter drilled shafts for Northumberland Strait bridge project. *Can. Geotech. J.*, Ottawa, 34, 580–587.

Wilson L. C. 1976. Tests of bored and driven piles in cretaceous mudstone at Port Elizabeth, South Africa. *Geotechnique*, London, 26, 5–12.

Zhang L. and Einstein H. H. 1998. End Bearing Capacity of Drilled Shafts in Rock. *Journal of Geotechnical and Geoenvironmental Engineering*, 124(7), 574–584.

Zhang L. and Einstein H.H. 1999. Closure to end bearing capacity of drilled shafts in rock. *J. Geotech. Eng.(ASCE)*. 125(12), 1109-1110.